

# Spectroscopic characterization and detection of Ethyl Mercaptan in Orion <sup>1</sup>

L. Kolesníková

*Grupo de Espectroscopía Molecular (GEM), Edificio Quifima, Laboratorios de Espectroscopía y Bioespectroscopía, Parque Científico UVa, Unidad Asociada CSIC, Universidad de Valladolid, 47005 Valladolid, Spain.*

lucie.kolesnikova@uva.es

and

B. Tercero and J. Cernicharo

*Departamento de Astrofísica, Centro de Astrobiología CAB, CSIC-INTA, Ctra. de Torrejón a Ajalvir km 4, 28850 Madrid, Spain.*

terceromb@cab.inta-csic.es, jcernicharo@cab.inta-csic.es

and

J. L. Alonso and A. M. Daly

*Grupo de Espectroscopía Molecular (GEM), Edificio Quifima, Laboratorios de Espectroscopía y Bioespectroscopía, Parque Científico UVa, Unidad Asociada CSIC, Universidad de Valladolid, 47005 Valladolid, Spain.*

jlalonso@qf.uva.es, adammichael.daly@uva.es

and

B. P. Gordon and S. T. Shipman

*Division of Natural Sciences, New College of Florida, Sarasota, FL 34243, USA.*

brittany.gordon@ncf.edu, shipman@ncf.edu

## Abstract

New laboratory data of ethyl mercaptan,  $\text{CH}_3\text{CH}_2\text{SH}$ , in the millimeter and submillimeter-wave domains (up to 880 GHz) provided very precise values of the spectroscopic constants that allowed the detection of *gauche*- $\text{CH}_3\text{CH}_2\text{SH}$  towards

Orion KL. 77 unblended or slightly blended lines plus no missing transitions in the range 80 – 280 GHz support this identification. A detection of methyl mercaptan,  $\text{CH}_3\text{SH}$ , in the spectral survey of Orion KL is reported as well. Our column density results indicate that methyl mercaptan is  $\simeq 5$  times more abundant than ethyl mercaptan in the hot core of Orion KL.

*Subject headings:* ISM: abundances — ISM: individual objects (Orion KL) — ISM: molecules — line: identification

## 1. Introduction

The spectral millimeter-wave survey of Orion KL carried out with the IRAM 30m radio telescope presented more than 8000 unidentified lines (Tercero et al. 2010; Tercero 2012). Many of them (nearly 4000) have been identified as lines arising from isotopologues and vibrationally excited states of abundant species (Demyk et al. 2007; Carvajal et al. 2009; Margulès et al. 2009, 2010; Tercero et al. 2012; Motiyenko et al. 2012; Daly et al. 2013; Coudert et al. 2013; Haykal et al. 2013b, A. López et al. in preparation). These identifications significantly reduce the number of U-lines and mitigate line confusion in the spectra. Nevertheless, many of those features still remain unidentified. Therefore, a search for new molecular species in that cloud based on precise laboratory measurements continues to be a field of a great research activity. Recently, the discovery of methyl acetate and *gauche*-ethyl formate (Tercero et al. 2013), the search for allyl isocyanide (Haykal et al. 2013a) as well as a tentative detection of phenol (Kolesniková et al. 2013) have been reported.

Methanol and ethanol are very well known molecules in many astrophysical environments. The thiol equivalent of methanol, methyl mercaptan ( $\text{CH}_3\text{SH}$ ), has been detected towards Sgr B2 by Linke et al. (1979). Previous searches for it towards dark clouds and Orion did not provide positive results (Irvine et al. 1987, 1989). However, this molecule has been recently detected towards the cold first hydrostatic core B1 (Cernicharo et al. 2012) and was also observed towards the hot core G327.3-0.6 by Gibb et al. (2000). Hence, the thiol equivalent of ethanol, ethyl mercaptan ( $\text{CH}_3\text{CH}_2\text{SH}$ ), could also be present in space. Initial studies of the Stark modulated microwave spectra by Imanov et al. (1967), Hayashi et al. (1970), Hayashi et al. (1973), Quade et al. (1975), and Nakagawa et al. (1976) provided the

---

<sup>1</sup>This work was based on observations carried out with the IRAM 30-meter telescope. IRAM is supported by INSU/CNRS (France), MPG (Germany) and IGN (Spain).

first values of the spectroscopic constants for the *gauche* and *trans* conformers of ethyl mercaptan. These microwave laboratory data, however, cannot be used to accurately predict their frequencies in the millimeter and submillimeter-wave domains.

In this letter, we report new laboratory measurements of ethyl mercaptan in the millimeter and submillimeter-wave region and its first observation in the interstellar medium. Newly derived spectroscopic constants of its *gauche* and *trans* forms have allowed us to detect the *gauche* conformer towards Orion KL with the IRAM 30m radio telescope. *Trans*-ethyl mercaptan has been tentatively detected in this study. In addition, the first detection of methyl mercaptan towards Orion KL is also presented.

## 2. Laboratory Measurements

A commercial sample of ethyl mercaptan was used without any further purification. Rotational spectra in the 8.7 – 26.5 GHz region were taken at a temperature of  $-15\text{ }^{\circ}\text{C}$  and a pressure of 6 mTorr with a waveguide chirped-pulse Fourier transform microwave spectrometer at New College of Florida (Reinhold et al. 2011). The waveguide was cooled via a set of home-built cooling loops connected to a chiller with a recirculating fluid ( $-15\text{ }^{\circ}\text{C}$  is the base temperature reached). A 250 ns chirped pulse is generated with an arbitrary waveform generator (Tektronix AWG7101) and subsequently frequency shifted, filtered, and amplified before interacting with a static gas sample in a 10m coil of WRD-750 waveguide. The resulting molecular free induction decay is amplified and detected in the time-domain with an oscilloscope (Tektronix TDS6154C), after which it is Fourier transformed to generate a frequency-domain spectrum. In each spectrum, 2 million free induction decays of 4 microsecond duration were averaged and Fourier transformed using a Kaiser-Bessel window function. Peaks in the frequency-domain spectrum had a full width at half maximum of  $\sim 800\text{ kHz}$  and so the uncertainty on the line center was set to 80 kHz.

Rotational spectra in the millimeter (60 – 300 GHz) and submillimeter-wave (500 – 590 GHz, 625 – 660 GHz, and 835 – 880 GHz) regions were recorded at a pressure of approximately 15 mTorr by a recently constructed millimeter-wave spectrometer at the University of Valladolid (A. M. Daly et al. in preparation). The source of radiation is an Agilent E8257D synthesizer (250 kHz – 20 GHz) connected to a set of passive or active cascade frequency multipliers (VDI, Inc.). Room temperature measurements were carried out in a free space 360 cm long Pyrex cell. Up to 170 GHz, the optical path length was doubled using a rooftop mirror and a polarization grid. A silicon bolometer was used as the detection element above 800 GHz. At lower frequencies, the signal was detected by either Schottky diodes or the Quasi-optical broadband detectors (VDI, Inc.). All the spectra were recorded

in 1 GHz sections using the frequency modulation technique with second harmonic lock-in detection (modulation depth between 20 – 50 kHz and modulation frequency of 10.2 kHz for the semiconductor detectors and 90 Hz for the cryogenic detector). Frequency accuracy is estimated to be better than 50 kHz. Rotational spectra of the  $^{34}\text{S}$  isotopologue from the microwave up to the submillimeter-wave region were measured in natural abundance.

### 3. Rotational Spectra and Analysis

Ethyl mercaptan is a near prolate asymmetric top molecule which is present in two stable forms: *gauche* and *trans* configurations which are defined by the value of the torsion angle  $\alpha$  of the –SH group measured from the symmetry plane of the *trans* configuration ( $\alpha = 0$ ), see Figure 1-a. For the *gauche* conformer, two equivalent configurations at approximately  $\alpha = 120^\circ$  and  $240^\circ$  can be interchanged by tunneling motion. A schematic potential energy diagram for the –SH group torsion is shown in Figure 1-b. The tunneling process removes the vibrational degeneracy and the vibrational ground state is split into two substates labeled as  $0^+$  and  $0^-$  with an energy separation  $\Delta E = E^- - E^+$  of about 1750 MHz (Quade et al. 1975, Nakagawa et al. 1976). In order to facilitate the assignments of the *gauche*- and *trans*-ethyl mercaptan millimeter-wave spectra, the microwave data from Quade et al. (1975) were used for initial predictions of the rotational transitions. Pickett’s spectral fitting programs SPCAT and SPFIT (Pickett 1991) were used to predict the spectra as well as to determine the spectroscopic constants. The visualization, processing and the assignments of the rotational spectra were performed using the SVIEW and ASCP programs included in the AABS package (Kisiel et al. 2005).

The rotational spectrum of *gauche*-ethyl mercaptan is formed by two types of transitions: *a*- and *b*-type pure rotational transitions ( $|\mu_a| = 1.48$  (2) D,  $|\mu_b| = 0.19$  (10) D (Quade et al. 1975)) between the rotational levels within the same torsion substate, i.e.  $0^\pm \leftrightarrow 0^\pm$ , and *c*-type torsion-rotational transitions ( $|\mu_c| = 0.59$  (2) D (Quade et al. 1975)) connecting different torsion substates ( $0^\mp \leftrightarrow 0^\pm$ ). Figure 1-d illustrates a section of the *a*-type *R*-branch pure rotational transitions which are the dominant features of the ethyl mercaptan rotational spectrum. The doubling pattern of the *c*-type transitions resulting from the tunneling process can be seen in the Figure 1-e. The frequency separation between the corresponding *c*-type doublets is close to  $2\Delta E$ , which is about 3.5 GHz (see Figure 1-e).

Several near degeneracies of the  $0^+$  and  $0^-$  energy levels beginning at low  $J$  values have been observed which require accounting for the Coriolis-like terms that connect the  $0^+$  and  $0^-$  substates. Perturbation-allowed transitions between  $0^+$  and  $0^-$  energy levels with  $\Delta K_a = \text{even}$  and  $\Delta K_c = \text{even}$  selection rules arising from the mixing of the  $0^+$  and

$0^-$  substates with the same  $K_a$  quantum number have been observed as well. Finally, more than 2200 distinct transitions involving the rotational quantum numbers  $J''$  and  $K_a''$  up to 88 and 25, respectively, have been analyzed using the effective framework fixed axes two-state Hamiltonian as defined by Quade et al. (1963):

$$H_{\text{eff}} = H_{\text{rot}}^+ + H_{\text{rot}}^- + H^\pm + \Delta E, \quad (1)$$

where  $H_{\text{rot}}^+$  and  $H_{\text{rot}}^-$  represent the Watson’s  $A$ -reduced semirigid Hamiltonian in  $I^r$ -representation (Watson 1977) for the  $0^+$  and  $0^-$  substates, respectively, and  $H^\pm$  is the torsion-rotation interaction Hamiltonian:

$$H^\pm = D^\pm(J_b J_c + J_c J_b) + Q^\pm J_a + N^\pm J_b, \quad (2)$$

where  $D^\pm$ ,  $Q^\pm$ , and  $N^\pm$  represent the Coriolis-like coupling constants. Centrifugal distortion corrections up to the eighth order have been included in the analysis. All the perturbed transitions have been successfully treated by means of the Coriolis-like constants defined in Equation 2, with the  $K$ -dependence of  $D^\pm$  constant taken into account. For the *gauche*- $^{34}\text{S}$  isotopologue, more than 700 transitions ( $J''$  and  $K_a''$  up to 56 and 18, respectively) have been analyzed in the same manner as the parent species. The determined spectroscopic constants for both isotopologues are listed in Table 1. The measured frequencies are given in Table 2 (the full Table 2 is given in the Supplementary Material).

The rotational spectrum of *trans*-ethyl mercaptan is dominated by pure rotational  $a$ - and  $b$ -type transitions ( $|\mu_a| = 1.06$  (3) D,  $|\mu_b| = 1.17$  (3) D (Quade et al. 1975)). An example of measured  $a$ -type  $R$ -branch transitions is illustrated in Figure 1-c. Many assigned *trans* transitions with higher values of  $K_a''$  quantum numbers have been found to be affected by perturbations which may originate from interactions with low-lying first excited states of the  $-\text{SH}$  and  $-\text{CH}_3$  torsional modes. Only the unperturbed transitions were included in the final fit. More than 600 distinct transitions with  $J''$  and  $K_a''$  quantum numbers up to 64 and 13, respectively, were analyzed using the standard single-state semirigid  $A$ -reduced Hamiltonian (Watson 1977) with octic centrifugal distortion constants. The resulting spectroscopic constants are given in Table 1. The measured transitions are given in the full Table 2 (see the Supplementary Material).

#### 4. Astronomical Observations

Five observing sessions (from September 2004 to January 2007) were required for completing a molecular line survey in all the frequencies available by the A, B, C, and D receivers (80 – 115.5, 130 – 178, 197 – 281 GHz) of the IRAM 30m telescope towards Orion KL (IRc2

source at  $\alpha(\text{J2000})=5^h 35^m 14.5^s$ ,  $\delta(\text{J2000})=-5^\circ 22' 30.0''$ ). System temperatures, image side band rejections, and half power beam widths were in the ranges 100 – 800 K, 27 – 13 dB, and 29 – 9", respectively, from lower to higher frequencies. The intensity scale was calibrated using the ATM package (Cernicharo 1985; Pardo et al. 2001). The observations were performed in the balanced wobbler-switching mode. As backends we connected two filter banks (512 MHz of bandwidth for each one and 1 MHz of spectral resolution) and a correlator (2×512 MHz of bandwidth and 1.25 MHz of spectral resolution). Pointing and focus were checked every 1 – 2 hours on nearby quasars. The data were processed with the GILDAS software<sup>2</sup>. The data reduction consisted of removing lines from the image side band and fitting and removing baselines. Figures are shown in units of main beam temperature,  $T_{MB}=T_A^*/\eta_{MB}$ , where  $\eta_{MB}$  is the main beam efficiency. More detailed description of the observations can be found in Tercero et al. (2010).

At least four cloud components could be identified in the line profiles of our low resolution spectral lines, characterized by different radial velocities and line widths (Blake et al. 1987; Schilke et al. 2001; Persson et al. 2007; Tercero et al. 2010, 2011; Neill et al. 2013). Each component corresponds to a specific region of the cloud that overlaps in our telescope beam: the extended ridge or ambient cloud ( $T_K \simeq 60$  K); the compact ridge, a dense clump characterized by the emission of organic saturated O-rich molecules at a  $T_K \simeq 150$  K; the plateau, or outflow from the new born stars ( $T_K \simeq 150$  K); and the hot core, a dense and warm region rich in organic saturated N-bearing molecules ( $T_K \simeq 250$  K).

## 5. Results and Discussion

Direct laboratory measurements and derived spectroscopic constants given in Table 1 have allowed us to detect *gauche*-ethyl mercaptan and to tentatively detect the *trans* conformer in the molecular line survey of Orion KL by means of a large number of spectral lines free of blending with other species. Table 2 provides (together with the transitions measured in the laboratory) the observational parameters of the detected lines that are not strongly blended with other molecules. Owing to the weakness of these features, the main beam temperature has been obtained from the peak channel of the spectra, so errors in the baselines and contribution from other species could affect this parameter. Therefore,  $T_{MB}$  has to be considered as the total intensity of the detected feature and an upper limit to the intensity of ethyl mercaptan in this study. A total amount of 34 transitions free of blending (in the peak channel of the feature) and 43 slightly blended lines are reported in

---

<sup>2</sup><http://www.iram.fr/IRAMFR/GILDAS>

Table 2 for *gauche*-ethyl mercaptan. No missing lines have been found for this conformer. Figure 2 shows some of the lines of *gauche*-ethyl mercaptan reported here. Even though the *gauche* conformer being more stable, the number of potential lines to be detected for the *trans* conformer could be larger due to the higher value of its *b*-dipole moment component (see above). For *trans*-ethyl mercaptan, 72 lines free of blending and 52 slightly blended lines could be present in the survey. They are listed in Table 2 with the estimate of their parameters. However, the weakness of the transitions of *trans*-CH<sub>3</sub>CH<sub>2</sub>SH and the high overlap with other molecules make difficult the assignment of isolated lines of this conformer as they appear at the confusion limit of the line survey. Hence, we consider only a tentative detection for the *trans* conformer of ethyl mercaptan (see below). We also searched for CH<sub>3</sub>CH<sub>2</sub>SH in the PRIMOS survey<sup>3</sup> with the Green Bank Telescope (GBT) in the frequency range between 300 MHz and 50 GHz and in the  $>13\sigma$  U lines of the 3 mm IRAM 30m survey reported by Belloche et al. (2013), both surveys towards SgrB2, finding a negative detection in both set of data.

In order to compare the emission of ethyl mercaptan with that of methyl mercaptan, the latter species was searched for in Orion KL. The laboratory frequencies and dipole moment values used for the methyl mercaptan are those predicted by Bettens et al. (1999) and have been implemented in the MADEX code (Cernicharo 2012). Figures 2 and 3 show selected lines of *gauche*-CH<sub>3</sub>CH<sub>2</sub>SH and A/E-CH<sub>3</sub>SH, respectively. Both Figures show our best model for these species (see below), and the total model for the already studied species in this survey (see Tercero et al. 2013 and references therein). The figures show lines free of blending, or moderately blended with lines from other species. No missing lines have been found for methyl mercaptan in the frequency range covered by our line survey.

To model the emission of A/E-CH<sub>3</sub>SH and *gauche/trans*-CH<sub>3</sub>CH<sub>2</sub>SH we have considered that both molecules come from the same region of Orion KL (hot core at  $v_{LSR} = 5 \text{ km s}^{-1}$  and  $\Delta v = 7 \text{ km s}^{-1}$ ). Lines from methyl mercaptan are typically 10 times stronger than those of ethyl mercaptan. We used the MADEX code in LTE conditions due to the lack of collisional rates for these species. Beam dilution and the position of the source with respect to the pointing position were taken into account in our models. We assumed a  $d_{sou} = 10''$  and  $offset = 3''$ . In Tercero et al. (2010) we estimated the uncertainties of the column density results in this survey to be between 20 – 30 % considering different sources of uncertainty such as the spatial overlap of the different cloud components, the modest angular resolution of any single-dish line survey or pointing errors. Nevertheless, the uncertainty due to high overlap problems has to be considered for results obtained by means of weak

---

<sup>3</sup>Hollis, J. M.; Remijan, A. J.; Jewell, P. R.; Lovas, F. J.; Corby, J. F. <http://www.cv.nrao.edu/~aremijan/PRIMOS/index.html>

lines such as those of ethyl mercaptan (raising the uncertainty up to 50 %). The physical and chemical parameters derived by the model are a common kinetic temperature of  $200\pm 50$  K for ethyl and methyl mercaptan and a column density of  $(5.0\pm 2.0)\times 10^{15}$  cm<sup>-2</sup> for each A and E state of CH<sub>3</sub>SH and of  $(2.0\pm 1.0)\times 10^{15}$  cm<sup>-2</sup> for *gauche*-ethyl mercaptan. For *trans*-CH<sub>3</sub>CH<sub>2</sub>SH we can report only a tentative detection with an upper limit to its column density of  $\leq(2.0\pm 1.0)\times 10^{15}$  cm<sup>-2</sup>. Therefore, we found that methyl mercaptan is  $\simeq 5$  times more abundant than ethyl mercaptan in the hot core of Orion KL. The population of different conformers of CH<sub>3</sub>CH<sub>2</sub>SH follows a Boltzmann distribution so the abundance ratio between both conformers of ethyl mercaptan is given by  $N(\textit{trans})/N(\textit{gauche}) = \exp(-E_{rel}/T_k)$ , where  $E_{rel}$  is the difference of energy between the conformers (230 K, M. L. Senent, private communication) and  $T_k$  is the kinetic temperature of the medium. At 200 K this formula yields a  $N(\textit{trans})/N(\textit{gauche})$  value of 0.32 whereas at 300 K this number rises up to 0.46. These abundance ratios have to be corrected by the vibrational partition function of both conformers. For  $T_K=200$  K the vibrational partition function for *gauche* is 1.47 and for *trans* it is 1.54 (M. L. Senent, private communication). Applying these corrections, our abundance ratio between *trans* and *gauche* (both states 0<sup>+</sup> and 0<sup>-</sup>) is  $\leq 1$ .

In order to compare these results with structurally similar molecules, we modeled the emission of ethanol (*trans/gauche*-CH<sub>3</sub>CH<sub>2</sub>OH) and methanol (A/E-<sup>13</sup>CH<sub>3</sub>OH) in our line survey using the MADEX code and LTE conditions (A. López et al., in preparation). For fitting the line profiles in this large spectral range, five cloud components are required: the four components described in Sect. 4 and a hotter (300 K) and smaller ( $d_{sou}=7''$ ) compact ridge. For the four former components, the assumed physical conditions are those derived in Tercero et al. (2010). We obtained a column densities of  $(6\pm 2)\times 10^{17}$  cm<sup>-2</sup>,  $(2.2\pm 0.6)\times 10^{16}$  cm<sup>-2</sup>, and  $(1.7\pm 0.4)\times 10^{16}$  cm<sup>-2</sup> for each state of CH<sub>3</sub>OH (assuming a <sup>12</sup>C/<sup>13</sup>C ratio of 45, see Tercero et al. 2010), for the *trans* conformer of ethanol, and for *gauche*-CH<sub>3</sub>CH<sub>2</sub>OH, respectively. Therefore, methanol is 30 times more abundant than ethanol in Orion KL. This difference between  $X(\text{CH}_3\text{OH}/\text{CH}_3\text{CH}_2\text{OH})$  and  $X(\text{CH}_3\text{SH}/\text{CH}_3\text{CH}_2\text{SH})$  could be due to the methanol and methyl mercaptan stay time on the dust grains before evaporation. If methyl mercaptan stays on the dust grains longer time than methanol, then, further chemical processing could occur changing the abundance ratios between methyl and ethyl species. Taking into account that the emission of the -OH species comes mainly from the compact ridge whereas methyl and ethyl mercaptan emit from the hot core, the differences of relative abundances between the methyl and ethyl species could be also due to the chemical differentiation between these two regions inside Orion KL. Most sensitive observations, with interferometers such us ALMA are needed to derive accurate column densities of the two conformers of ethyl mercaptan and to study their spatial distribution in Orion.



The authors thank the Spanish MINECO for support under grants AYA 2009-07304, AYA2011-29375, CTQ 2006-05981/BQU, CTQ 2010-19008, and the CONSOLIDER program "ASTROMOL" CSD 2009-00038 and Junta de Castilla y Leon (Grant VA070A08). B.P.G. and S.T.S. acknowledge support from the National Science Foundation Division of Chemistry under Grant No. 1111101 (co-funded by MPS/CHE and the Division of Astronomical Sciences) and B.P.G. also thanks New College of Florida for a Student Research and Travel Grant award.

## REFERENCES

- Blake, G. A., Sutton, E. C., Masson, C. R., & Philips, T. H. 1987, *ApJ*, 315, 621
- Belloche, A., Müller, H. S. P., Menten, K. M., Schilke, P. & Comito, C. 2013, *A&A*, 559, 47
- Bettens, F.L., Sastry, K.V.L.N, Herbst, E., et al., 1999, *ApJ*, 510, 789
- Carvajal, M., Margulès, L., Tercero, B., et al. 2009, *A&A*, 500, 1109
- Cernicharo, J. 1985, Internal IRAM report (Granada: IRAM)
- Cernicharo, J., 2012, in *ECLA-2011: Proceedings of the European Conference on Laboratory Astrophysics*, EAS Publications Series, 2012, Editors: C. Stehl, C. Joblin, & L. d’Hendecourt (Cambridge: Cambridge Univ. Press), "Laboratory astrophysics and astrochemistry in the Herschel/ALMA era", 58, 251
- Cernicharo, J., Marcelino, N., Roueff, E., et al., 2012, *ApJ*, 759, L43
- Cernicharo, J., Tercero, B., Fuente, A., et al. 2013, *ApJ*, 771, L10
- Coudert, L. H., Drouin, B. J., Tercero, B., et al. 2013, *ApJ*, 779, 119
- Daly, A. M., Bermúdez, C., López, A., et al. 2013, *ApJ*, 768, 81
- Demyk, K., Mäder, H., Tercero, B., et al. 2007, *A&A*, 466, 255
- Gibb, E., Nummelin, A., Irvine, W.M., et al., 2000, *ApJ*, 545, 309
- Hayashi, M., Imaishi, H., Ohno, K., & Murata, H. 1971, *Bull. Chem. Soc. Jap.*, 44, 872
- Hayashi, M., Imaishi, H., & Kuwada, K. 1973, *Bull. Chem. Soc. Jap.*, 47, 2382
- Haykal, I., Margulès, L., Motiyenko, R. A. et al. 2013, *ApJ*, 777, 120

- Haykal, I., Carvajal, M., Tercero, B. et al. 2013, A&A submitted
- Imanov, L. M., Qajar, Ch. O., & Abbasov, A. A. 1967, Phys. Lett., 34A, 485
- Irvine, W.M., Goldsmith, P.F., Hjalmarson, A., 1987, in *Interstellar Processes*, Ed. P.J. Hollenbach & H.A. Thronson (Dordrecht: Reidel), 561
- Irvine, W.M., Friberg, F., Kaifu, N. et al., 1989, ApJ, 342, 871
- Kisiel, Z., Pszczolkowski, L., Medvedev, I. R., et al. 2005, JoMoSp, 233, 231
- Kolesniková, L., Daly, A. M., Alonso, J. L., Tercero, B., & Cernicharo, J. 2013, JoMoSp, 289, 13
- Linke, R.A., Frerking, M.A., Thaddeus, P., 1979, ApJ, 234, L139
- Margulès, L., Motiyenko, R. A., Demyk, K., et al. 2009, A&A, 493, 565
- Margulès, L., Huet, T. R., Demaison, J., et al. 2010 ApJ, 714, 1120
- Motiyenko, R. A., Tercero B., Cernicharo, J., & Margulès, L. 2012, A&A, 548, A71
- Nakagawa, J., Kazunori, K., & Hayashi, M. 1976, Bull. Chem. Soc. Jap., 49, 3420
- Neill, J. L., Crockett, N. R., Bergin, E. A., Pearson, J. C. & Xu, L-H. 2013, ApJ, 777, 85
- Pardo, J. R., Cernicharo, J., & Serabyn, E. 2001, IEEE Trans. Antennas and Propagation, 49, 12
- Persson, C. M., Olofsson, A. O. H., Koning, N., et al. 2007, A&A 476, 807
- Pickett, H. M. 1991, JoMoSp, 148, 371
- Quade, C. R. & Lin, C. C. 1963, JCP, 38, 540
- Quade, C. R. & Schmidt, R. E. 1975, JCP, 62, 3864
- Reinhold, B., Finneran, I. A., & Shipman, S. T. 2011, JoMoSp, 270, 89
- Schilke, P., Benford, C. J., Hunter, T. R., Lis, D. C. & Philips, T. G. 2001, ApJS, 132, 281
- Schmidt, R. E. & Quade, C. R. 1975, JChPh, 62, 3864
- Tercero B., Cernicharo, J., Pardo, J. R., & Goicoechea, J. R. 2010, A&A, 517, 96
- Tercero B., Vincent L., Cernicharo, J., Viti S., & Marcelino N. 2011, A&A, 528, 26

Tercero, B. 2012, PhD, Univ. Complutense de Madrid

Tercero B., Margulès L., Carvajal, M., et al. 2012, A&A, 538, A119

Tercero, B., Kleiner, I., Cernicharo, J., et al. 2013, ApJ, 770, L13

Watson, J. K. G. 1977, in *Vibrational Spectra and Structure*, Vol. 6, ed. J. Durig (Amsterdam: Elsevier), 1

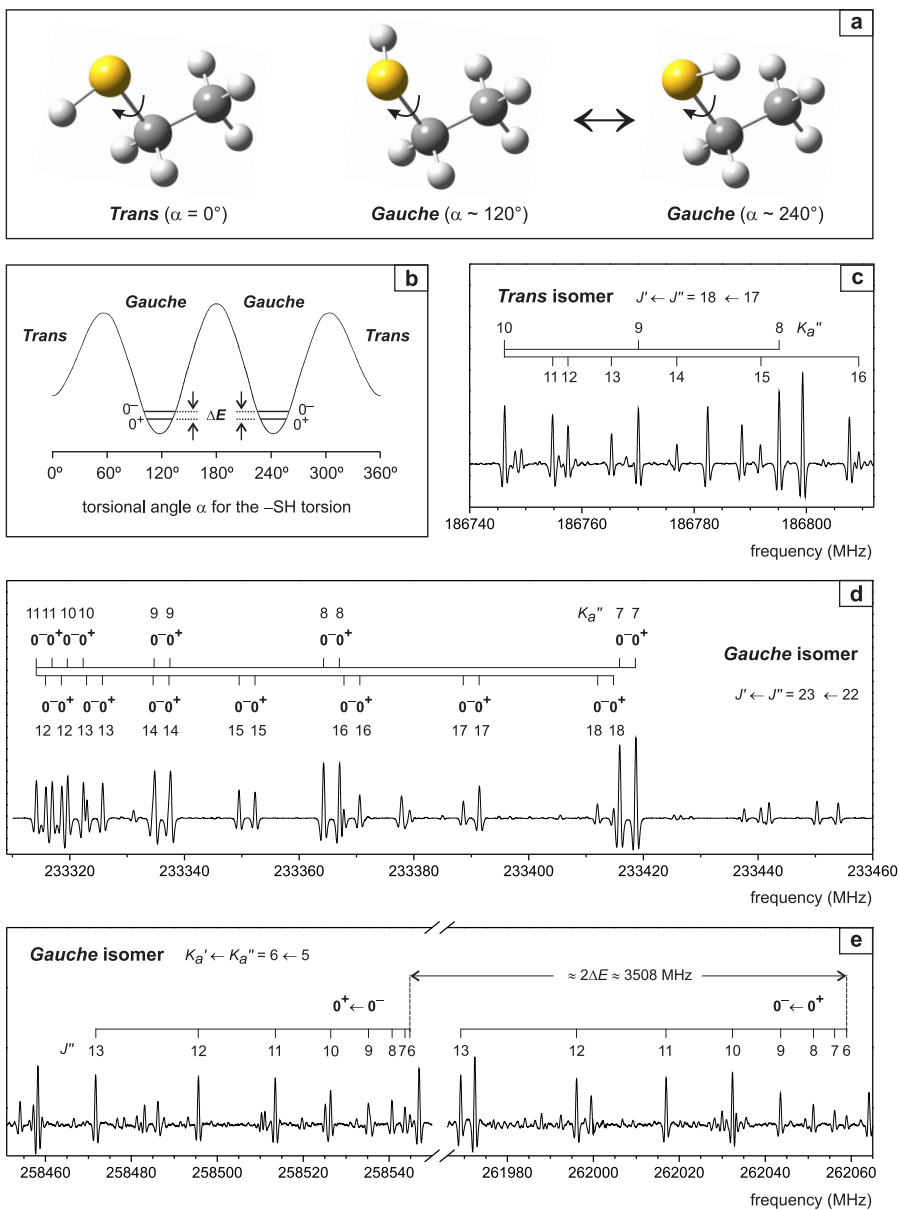


Fig. 1.— Ethyl mercaptan: (a) *trans* and two equivalent *gauche* configurations; (b) potential energy curve for the  $-SH$  group torsion with torsion sublevels for the *gauche* vibrational ground state; (c) *a*-type *R*-branch transitions of the *trans* isomer; (d) pure rotational *a*-type *R*-branch transitions of the *gauche* isomer; (e) torsion-rotational *c*-type  $Q$ -branch transitions of the *gauche* isomer.

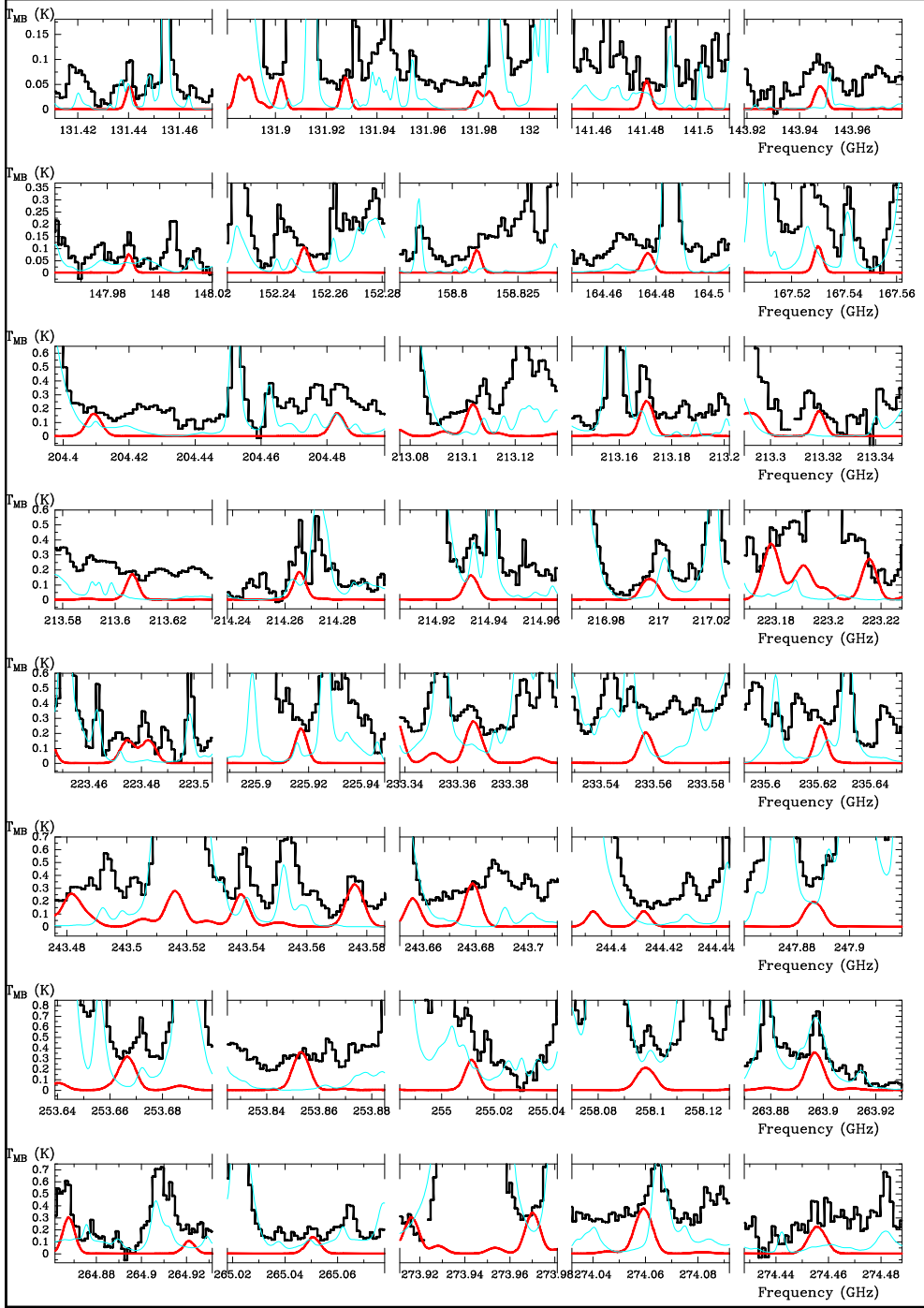


Fig. 2.— Selected lines of *gauche*-ethyl mercaptan towards Orion-IRc2 (in red). The continuous cyan line corresponds to all lines already modeled in our previous papers (see text). A  $v_{LSR}$  of  $5 \text{ km s}^{-1}$  is assumed.

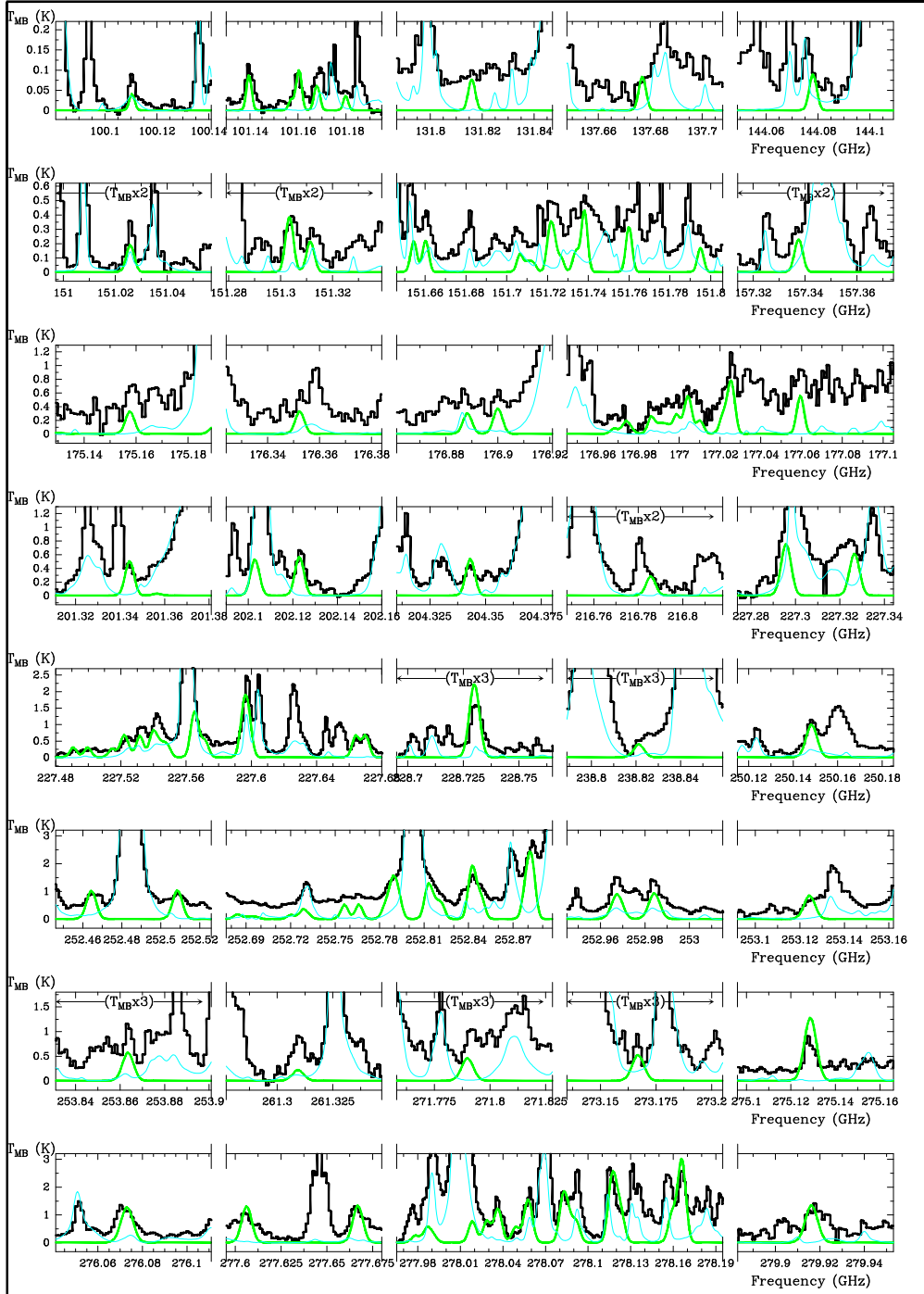


Fig. 3.— Selected lines of methyl mercaptan towards Orion-IRc2. The continuous cyan line corresponds to all lines already modeled in our previous papers (see text). A  $v_{LSR}$  of  $5 \text{ km s}^{-1}$  is assumed.

Table 1. Spectroscopic constants<sup>a</sup> of *gauche*- and *trans*-ethyl mercaptan (*A*-reduction, *I*<sup>r</sup>-representation).

Constant	Unit	<i>Gauche</i> (parent specie)		<i>Gauche</i> ( <sup>34</sup> S)		<i>Trans</i>
		0 <sup>+</sup>	0 <sup>-</sup>	0 <sup>+</sup>	0 <sup>-</sup>	
<i>A</i>	(MHz)	28747.4104 (66)	28747.2715 (65)	28709.699 (24)	28708.964 (26)	28416.7604 (18)
<i>B</i>	(MHz)	5295.1422 (36)	5295.0008 (36)	5175.5685 (36)	5175.4383 (36)	5485.77901 (15)
<i>C</i>	(MHz)	4845.9421 (36)	4845.9689 (36)	4744.7050 (36)	4744.7310 (36)	4881.81770 (15)
$\Delta_J$	(kHz)	3.326369 (20)	3.323582 (20)	3.18351 (18)	3.18084 (18)	3.83217 (27)
$\Delta_{JK}$	(kHz)	-18.39280 (60)	-18.35859 (60)	-17.9512 (15)	-17.8994 (14)	-22.4549 (58)
$\Delta_K$	(kHz)	204.1591 (82)	203.9217 (81)	206.8 (14)	205.1 (14)	210.03 (18)
$\delta_J$	(kHz)	0.514429 (12)	0.513170 (14)	0.481132 (82)	0.480129 (71)	0.65664 (11)
$\delta_K$	(kHz)	8.781 (12)	8.555 (12)	8.271 (34)	8.024 (35)	7.342 (20)
$\Phi_J$	(kHz)	0.0029872 (28)	0.0029225 (31)	0.0029872 <sup>b</sup>	0.0029225 <sup>b</sup>	-0.00086 (17)
$\Phi_{JK}$	(kHz)	0.0790 (13)	0.0661 (13)	0.0790 <sup>b</sup>	0.0661 <sup>b</sup>	0.367 (18)
$\Phi_{KJ}$	(kHz)	-1.3341 (45)	-1.2955 (44)	-1.3341 <sup>b</sup>	-1.2955 <sup>b</sup>	-2.717 (106)
$\Phi_K$	(kHz)	6.341 (48)	5.171 (46)	6.341 <sup>b</sup>	5.171 <sup>b</sup>	26.7 (80)
$\phi_J$	(kHz)	0.0012107 (15)	0.0011805 (16)	0.0012107 <sup>b</sup>	0.0011805 <sup>b</sup>	-0.000935 (91)
$\phi_{JK}$	(kHz)	0.04561 (63)	0.04326 (65)	0.04561 <sup>b</sup>	0.04326 <sup>b</sup>	-0.164 (26)
$\phi_K$	(kHz)	5.858 (95)	4.825 (97)	5.858 <sup>b</sup>	4.825 <sup>b</sup>	28.89 (97)
<i>L<sub>J</sub></i>	(mHz)	...	...	...	...	0.000060 (11)
<i>L<sub>KKJ</sub></i>	(mHz)	...	...	...	...	2.11 (40)
<i>L<sub>K</sub></i>	(mHz)	-1.140 (75)	0.673 (71)	...	...	1374 (110)
<i>l<sub>JK</sub></i>	(mHz)	...	...	...	...	0.0497 (61)
<i>l<sub>KJ</sub></i>	(mHz)	0.0523 (38)	0.0414 (38)	...	...	4.77(50)
<i>l<sub>K</sub></i>	(mHz)	0.403 (21)	0.601 (19)	...	...	...
$\Delta E$	(MHz)	1753.9788 (37)	...	1730.995 (19)	...	...
<i>D</i> <sup>±</sup>	(MHz)	8.359 (96)	...	5.36 (14)	...	...
<i>Q</i> <sup>±</sup>	(MHz)	-15.00 (38)	...	-26.51 (57)	...	...
<i>N</i> <sup>±</sup>	(MHz)	6.30 (11)	...	...	...	...
<i>D<sub>K</sub></i> <sup>±</sup>	(MHz)	0.01358 (50)	...	...	...	...
$\sigma_{\text{fit}}$	(kHz)	39	...	41	...	30

<sup>a</sup>The numbers in parentheses are 1 $\sigma$  uncertainties in the units of the last decimal digit.

<sup>b</sup>Fixed to the parent species value.

Table 2. Laboratory measurements and astronomical detected lines of ethyl mercaptan.

$J'$	$K'_a$	$K'_c$	$v'$	$J''$	$K''_a$	$K''_c$	$v''$	Laboratory freq. (MHz)	Lab.–Pred. (MHz)	Conf.	$E_u$ (K)	$S_{ij}$	Sky Obs. freq. (MHz)	$T_{mb}$ (K)	Blend
13	5	8	1	12	5	7	1	131926.7036	-0.0205	G	72.8	11.1	131928.9	0.08	
13	5	9	1	12	5	8	1	131926.7036	0.0443	G	72.8	11.1	†		
13	5	8	0	12	5	7	0	131928.2800	-0.0229	G	72.7	11.1	†		
13	5	9	0	12	5	8	0	131928.2800	0.0420	G	72.7	11.1	†		
13	4	10	1	12	4	9	1	131978.8083	-0.0052	G	62.6	11.8	131977.9	0.07	
13	4	10	0	12	4	9	0	131980.4297	-0.0062	G	62.5	11.8	†		
13	4	9	1	12	4	8	1	131983.4352	-0.0123	G					
13	4	9	0	12	4	8	0	131985.0626	-0.0126	G					
13	3	11	1	12	3	10	1	132035.3178	-0.0038	G	54.6	12.3	132033.3	0.03	CH <sub>3</sub> COOCH <sub>3</sub>

Note. — This table is published in its entirety in the electronic edition of the *Astrophysical Journal Letters*. A portion is shown here for guidance regarding its form and content. Table gives the laboratory measurements and emission lines of the *gauche*- and *trans*-CH<sub>3</sub>CH<sub>2</sub>SH present in the Orion KL survey. All the transition frequencies included in the least-square analysis were weighted inversely proportional to the second power of their estimated uncertainties. The unresolved pairs of the asymmetry splitting were always included as two overlapped transitions and fitted to their intensity weighted averages. Columns 1–8 indicate the upper and lower state quantum numbers. Col. 9 gives the measured frequency at the laboratory. Col. 10 gives the difference between frequency measurements and predictions. Col. 11 gives the corresponding conformer. Col. 12 gives the upper level energy. Col. 13 gives the line strength. Col. 14 gives the observed frequency in the line survey of Orion assuming a  $v_{LSR}$  of 5 km s<sup>-1</sup>. Col. 15 gives the main beam temperature. Col. 16 indicates blended transitions with other molecules. † Blended with previous line.